

## Boise State University ScholarWorks

---

Civil Engineering Faculty Publications and  
Presentations

Department of Civil Engineering

---

1-26-2014

# Swell and Shrinkage Strain Prediction Models for Expansive Clays

Anand J. Puppala

*University of Texas at Arlington*

Thammanoon Manosuthikij

*University of Texas at Arlington*

Bhaskar C. S. Chittoori

*Boise State University*

---

NOTICE: this is the author's version of a work that was accepted for publication in *Engineering Geology*. Changes resulting from the publishing process, such as peer review, editing, corrections, structural formatting, and other quality control mechanisms may not be reflected in this document. Changes may have been made to this work since it was submitted for publication. A definitive version was subsequently published in *Engineering Geology*, (2013)] DOI: [10.1016/j.enggeo.2013.10.017](https://doi.org/10.1016/j.enggeo.2013.10.017).

# **Swell and Shrinkage Strain Prediction Models for Expansive Clays**

**By:**

**Anand J. Puppala, PhD, PE**

**(Corresponding Author)**

**Distinguished Teaching Professor**

**Tel # (817) 272-5821 and Fax # (817) 272-2630**

**Email: [anand@uta.edu](mailto:anand@uta.edu)**

**Thammanoon Manosuthikij, PhD**

**Former Doctoral Student**

**Department of Civil Engineering, Box 19308**

**The University of Texas at Arlington**

**Arlington, TX 76019, USA**

**Bhaskar, C. S. Chittoori, PhD, PE**

**Asst. Professor**

**Department of Civil Engineering**

**Boise State University**

**Boise, ID 83725**

**First Submission Date:**

**February 15, 2013**

**A Paper Submitted for Possible Publication in  
Engineering Geology**

## ABSTRACT

A comprehensive laboratory investigation was conducted to study volume change behaviors of five different types of expansive clayey soils sampled from various regions in Texas, USA. The laboratory test results, which were presented in an earlier paper, are analyzed here to evaluate existing correlations that can be used to predict swell and shrink-related displacements in these soils. The test database is also used to develop newer and practical models for predicting volume change-related soil properties. Models developed here used soil plasticity and compaction properties as independent variables. Newer models, that rely on seasonal compaction moisture content variations in the subsoils, were introduced to estimate both volumetric and vertical swell and shrinkage-induced soil deformations expected under civil infrastructure. The developed correlations, along with the existing models, were then used to predict vertical soil swell movements of four case studies where swell-induced soil movements were monitored. This comparison analysis showed that the model dependency on the volume change test procedural information and moisture content variation due to seasonal changes will lead to better prediction of swell movements in subsoils. Future research directions and recommendations are provided on implementation of the developed models in a realistic estimation of swell movements of infrastructure construction projects.

## INTRODUCTION

The first paper by Puppala et al. (2013) describes a comprehensive summary of testing programs and test results determined from five soil types sampled from various parts of Texas. All five soils, containing different amounts of expansive clay minerals, were subjected to swell, shrinkage and suction-based characterization tests. All these tests were conducted at different compaction moisture content and dry unit weight conditions.

The main intent of the comprehensive testing program was to develop an understanding of the effectiveness of various available models to provide realistic predictions of vertical or

volume change behaviors of expansive soils when subjected to seasonal changes. Newer prediction models were introduced or developed for better interpretation of volume changes in expansive soils. An attempt was specifically made to develop these models for shrinkage environmental conditions, which is currently lacking in the expansive soil characterization.

Analyses of the present test results are attempted in two sections. The first section focuses on evaluating the ability of the test database to analyze existing models, based on soil properties, and to predict volume changes in expansive soils. Also, new correlations are developed for both volumetric and vertical strains in swell and shrinkage environments as a function of moisture content variation in field conditions.

In the second section, a few models, including the ones developed from this research, are fully evaluated to predict volume change properties of expansive soils. This analysis focuses on volume change prediction models for soils subjected to swell conditions. Predictions and comparisons with field elevation measurements provided explanations on the capabilities of the models to make a realistic estimation of swell-induced volume changes. Also, future research directions on this topic, as well as implementation guidelines of the correlations to provide accurate prediction of volume change properties of expansive subsoils are explained.

## **ANALYSES OF TEST RESULTS**

As noted earlier, the present analysis is presented in two sections. The first section describes the analyses of test data into various relationships and compares them with existing models. Also, a few new models for predicting volume changes in expansive soils are introduced, and these models rely on compaction moisture content changes that transpire during seasonal changes. In the second section, a few models, including newly developed models, are

evaluated for predictions of swell-induced volume changes in four case studies where swell-induced displacements are fully monitored. Analyses of these models provided insights into the capabilities of these models for their prediction of swell-induced soil movements on pavement infrastructure. The geotechnical and mineralogical properties of the soils tested in this research are presented in Table 1, while the soil swelling movements, based on the empirical correlations from the laboratory data, are presented in Table 2.

## **TEST DATA ANALYSIS AND CORRELATION DEVELOPMENT**

### **Relationships Between Vertical and Volumetric Swell Strains**

Potential Vertical Rise (PVR), a method developed by the Texas Department of Transportation (TxDOT), has been widely used to estimate swell-related volume changes that have occurred in expansive soils. This PVR model was based on several assumptions, and one of them is that the vertical swell strain is equivalent to one-third of the volumetric swell strain of the soil at different overburden depths. This assumption needs to be closely evaluated, as this PVR model is known to provide misleading estimations of volume changes of soils with different plasticity properties. Hence, the assumption of vertical swell strain close to 33% of volumetric swell strain needs to be examined, as this assumption was based on free swell tests conducted in plane strain type 1-D swell tests. The present experimental program utilized three-dimensional swell strain tests, and these results are used in the present evaluations.

Swell strains of vertical and volumetric components of all five tested soils are presented in Figure 1a. All test results showed similar slopes between vertical and volumetric swell strain test results. This ratio of vertical (or axial) strain to volumetric strain is termed as Axial to Volumetric Strain Ratio (AVSR), and this term is expressed in real numbers, with no units. The

measured data is slightly scattered; nevertheless, this data yielded an average slope value close to 0.51. This value is significantly different from the 0.33 (or 1/3) typically used in the PVR prediction models based on soil elasticity theories. Expansive soils of shallow depths exhibit considerable lateral swell strains, which contributes to the final volumetric swell strain. Also, the present three-dimensional swell strain test methodology captures true response of swell behavior of expansive soils at shallow depths when compared to one-dimensional free swell tests. Thus, it is recommended that the constant parameter used in the PVR model be revised for better estimation of swell strain potentials of expansive soils.

Figure 1b illustrates the influence of the plasticity index (PI) of the soil on the AVSR test results. There is no variation in the AVSR magnitudes of various soils with distinct PIs, indicating that one AVSR value can be used for all expansive soil types of different plasticity values. From the present study results, a constant AVSR value of 0.5 is recommended for all soils to convert volumetric swell strains to vertical swell strains.

### **Relationships Between Vertical and Volumetric Strains – Shrinkage Environment**

Present volumetric shrinkage strain test data was also analyzed by plotting vertical shrinkage strain against volumetric shrinkage strains, and these results are presented in Figure 2a. The slopes of the strains (AVSR) were determined, and these results are graphically presented against the PI values in Figure 2b. The AVSR patterns for shrinkage strains were somewhat similar to those of swell strains. The AVSR magnitudes varied from 0.25 to 0.38, with the low value measured for Houston clayey soil. The mean value of these AVSRs for all soils was close to 0.35, which is significantly less than the average AVSR values of swell strain results.

Overall, it is shown that the radial shrinkage strain is larger than the radial swelling strain for the same amount of volumetric strain of an expansive soil. This explains the reasons behind pavement cracking, which often occurs in the dry summer season and/or high shrinkage conditions. These cracks will become worse with prolonged exposure of drying conditions and are also known to increase with seasonal wetting and drying periods. It is also interesting to note that the shrinkage pattern of expansive soil is different than the swelling pattern, showing that the changes in volumetric strains do not necessarily follow the same trends in both swell and shrinkage environments. The following sections describe studies that evaluate the existing correlations of swell strains that are based on Plasticity Index (PI) property.

### **Plasticity Index Based Correlations**

Test data from the present 3-D free swell strain tests of all soils were plotted against the plasticity index property of the same soils to develop PI-based empirical models for predicting swell strain potentials of expansive clayey soils. The experimental data was grouped into three different compaction moisture content conditions; namely, wet of optimum (WOPT), optimum (OPT) and dry of optimum (DOPT) moisture contents. An attempt was made in this figure to correlate measured vertical, radial and volumetric swell strains with the PI values. These results are presented in Figures 3, 4 and 5, respectively. These relationships are described by simple empirical equations as indicated in the Figures 3 to 5. Most of the relationships derived in the figures show good-to-strong relationships between volumetric swell strains and PI values.

There are several laboratory-based swell strain and plasticity index correlations derived from the literature. Two correlations developed by Seed et al. (1962) and Chen (1983) are described here. The first correlation was developed by Seed (1962) and is presented in the following:

$$\varepsilon_{s,ver} = \frac{\Delta h}{h} (\%) = 60 \times K \times PI^{2.44} \quad (1)$$

Where  $K = 3.6 \times 10^5$  and  $PI =$  Plasticity Index.

The second correlation was introduced by Chen (1983) and is presented in the following:

$$\varepsilon_{s,ver} = \frac{\Delta h}{h} (\%) = B \times e^{A \times PI} \quad (2)$$

Where  $A = 0.0838$  and  $B = 0.2558$ .

The third correlation was developed from the present test results and this equation was derived from the present tests conducted at optimum moisture content conditions. This correlation is presented in the following:

$$\varepsilon_{s,ver} = \frac{\Delta h}{h} (\%) = 0.0148 \times PI^{1.415} \quad (3)$$

All three correlations were used to predict the vertical swell strains of present test soils using the laboratory independent properties, and these results are presented in Figure 6. The present correlation is in agreement with two correlations developed by Seed et al. (1962) and Chen (1983). The first correlation provided slightly upper-bound prediction results when compared to the present research results; whereas, the second correlation yielded lower bound prediction results.

This variation is attributed to the following procedural-related information on swell characterization studies. The correlation proposed by Seed et al. (1962) was derived from one-dimensional swell test results with no seating pressure conditions; whereas, Chen's correlation was derived based on the test results obtained from swell tests by applying a moderate seating pressure. The present correlation, which allowed lateral soil movements and tested with no seating load or pressures, appears to follow somewhere in between them.



It is clear that the swell strain potential of a soil specimen is dependent on both lateral boundary condition and the amount of seating pressure magnitudes. A moderate amount of seating pressure can suppress swell potentials however, rigid wall test setups where no lateral movement is allowed (typically simulated in oedometer test setup) could result in higher swell potentials than the setup that allows movement in lateral direction. Hence the previous correlations are expected to represent both upper and lower boundary swell strain limits, and the present correlation is expected to fall within the correlation predictions. This explanation is in agreement with the results reported in Figure 6.

### **PI Based Shrinkage Strain Correlations**

Currently, no models are available in the literature to predict shrinkage strain potentials of expansive soils. Hence, an attempt is made to develop correlations between laboratory-based shrinkage strain measurements and PI properties of present soils. In this analysis, radial, vertical and volumetric shrinkage strain data from present soils tested at three compaction moisture content conditions are considered and used. Figures 7 and 8 present both vertical and volumetric shrinkage strains of all five soils, versus the PI of the soils at various moisture content state conditions. Both correlations developed have yielded high coefficients of determination values, suggesting that these are good correlations.

Also, results indicate that both volumetric and vertical shrinkage strains show a strong dependency of the PI value, and this trend appeared to display non-linear behavior. Overall, the trends show that more soils with different PI values than those covered in this research would be needed to enhance the developed shrinkage strain correlations. Nevertheless, the trends obtained here show that these correlations can be used to estimate approximate vertical or volumetric shrinkage strains of clayey soils compacted at different moisture conditions.

## Relationships Between PI and Percent Montmorillonite

The plasticity index or PI of a soil indirectly relates the expansive activity of a particular soil since the higher the plasticity index, the higher the potential to absorb moisture content. Montmorillonite is an expansive clay mineral with a very high PI value. The PI of a pure Montmorillonite soil can be as high as 514, which is regarded as a highly expansive soil (Fahoum, 1996). Hence an attempt is made to correlate the percent of the Montmorillonite clay mineral in the soil with the plasticity index (PI) value of the present soils. Figure 9 presents this relationship. The  $R^2$  value of this correlation is 0.77, indicating that a reasonably good correlation has been obtained between these two parameters. This relationship can be indirectly used to characterize the expansive soils. However, it should be noted that soft soils that exhibit similar plasticity properties, and hence characterization beyond the plasticity index property, are needed for understanding swell-shrink potentials of expansive soils.

## New Correlations Based on Moisture Content Changes ( $\Delta w$ )

Kodikara (2006) showed that the relationships between the volumetric shrinkage or swell strains ( $\varepsilon_{vol, swell/shr}$ ) and the reduction in compaction moisture content ( $\Delta w$ ) observed during shrinkage tests follow a linear correlation. These correlations are valid for slurry and compacted clayey specimens. The relationship can be expressed in the following form:

$$\varepsilon_{vol, swell/shr} = \alpha \times \Delta w \quad (4)$$

Where  $\alpha$  = Volumetric swell/shrinkage coefficient;  $\Delta w$  = change in compaction moisture content.

An attempt was made to correlate volumetric and vertical strains in both swell and shrinkage conditions, with the corresponding moisture content change recorded during the respective test. Figures 10 and 11 present these results for both swell and shrinkage strains,

respectively, along with their formulations and coefficients of determination values. Good correlations for both swell (Eqs 5 to 7) and shrinkage (Eqs 8 to 10) strains of soils with moisture content changes are obtained, and these are presented in the following equations:

$$\varepsilon_{s,vol} = 0.70 \times \Delta w \quad (5)$$

$$\varepsilon_{s,ver} = 0.36 \times \Delta w \quad (6)$$

$$\varepsilon_{s,rad} = 0.15 \times \Delta w \quad (7)$$

$$\varepsilon_{sh,vol} = 0.66 \times \Delta w \quad (8)$$

$$\varepsilon_{sh,ver} = 0.23 \times \Delta w \quad (9)$$

$$\varepsilon_{sh,rad} = 0.23 \times \Delta w \quad (10)$$

As noted in the above equations, soil volumetric, vertical and radial changes are expressed as functions of moisture content changes regardless of the soil types and initial moisture conditions. A few of these correlations have low  $R^2$  values, and these correlation predictions should be carefully assessed. Nevertheless, the correlations development as functions of moisture content changes represent a significant step since one can correlate swell and shrinkage strain movements as functions of moisture content changes that have transpired from swell or shrinkage conditions from seasonal changes.

The developed correlations are valid for the soil types that are utilized in this analysis. Further and future validation studies with new soil data will refine these correlations and enhance the reliability in these correlations.

## **VALIDATION ANALYSIS OF SWELL STRAIN PREDICTION MODELS**

In this section, several swell strain prediction models in the literature, along with the present moisture content based model and one numerical model, were analyzed to predict soil

swell movements for four pavement test sites that have distinct soil types, with different field conditions. Three analytical vertical swell strain prediction models developed by Hamberg (1985), PVR Method by McDowell (1956), and Lytton et al. (2004) were considered. Also, vertical swell prediction correlations that are dependent on moisture content variations were also considered for the same prediction analysis.

In addition, a numerical method-based Finite Element Method (FEM) was used to model the pavement section by employing a swell strain soil model. These model results were used to predict soil swell displacement experienced by the pavement sections. All these predictions are compared with field elevation measurements, and these comparisons are analyzed and discussed in the following sections.

### **Field Test Sites**

Four pavement test sites from Fort Worth, San Antonio, Paris and Houston, where in situ subgrades were instrumented with thermal and time domain transmissivity or TDT-based moisture content probes, were subjected to comprehensive field elevation monitoring of pavement test sections over a period of 24 months. Vertical swell strains from the field test sections were estimated from the maximum elevation changes observed over the period in which rainfall induced soil swelling occurred. These results were used, along with an assumed active depth of subsoil to determine total vertical swell strains. Typical active depths in Texas, USA vary from 0.9 to 3.0 m; hence, an average depth of 1.8 m is considered as a reasonable depth for the present analysis.

It should be noted that the same volumetric strain was used for comparisons with models that predict vertical swell strains, as vertical swell strains here simulated those transpired in 1-D

consolidation tests with rigid wall test setups. Hence the vertical strains measured can be considered as volumetric swell strains for those 1-D tests.

Figure 12 presents typical elevation changes that were observed at the Houston site. The monitored test data was used to extract the total volumetric swell strains in percent experienced by the pavement test sections. The swell movements were taken from the dip or valley in elevation data to a peak in the same data. This implies that this movement included a fraction of shrinkage-induced dip. The intent of this research work is to determine the maximum swell potential of soils from dry to wet conditions. Both peaks and valleys of the monitored curve are included in the determination of total vertical swell movements.

From monitored moisture probes, the moisture content fluctuations from dry to wet conditions were extracted and used in the analysis. In addition, comprehensive laboratory physical and engineering properties of the four test site soils were already available, as reported by Puppala et al. (2013), and these results were used in both the analytical and numerical models for the predictions of vertical swell strains.

### **Field Swell Strain Predictions**

As mentioned earlier, two different analytical models, PVR Method developed by McDowell (1956) and Lytton et al. (2004), were first evaluated. Both models used basic soil properties, including soil matric suction parameters, from Puppala et al. (2013) for the prediction analysis. Field moisture contents measured by TDT probes were then used to estimate moisture movements during seasonal changes, and this data was used in the present correlation for swell strain predictions.

### *FEM Model Predictions*

Numerical models, using FEM simulations, have been more accurate in depicting practical conditions more realistically than theoretical or analytical solutions based on infinite slab and other idealized assumptions (Kuo and Huang, 2006). A three-dimensional (3D) commercial software was used to study and model pavement behavior (Hammons 1998; Kim and Hjelmstad 2003); therefore, the same software was used in the present analysis.

For simulation of swell-related soil movements involving partially saturated soils, various advanced soil models that account for soil matric suction changes, volume changes of soils from moisture content fluctuations, and soil shear strength variations are needed. Such analysis is more challenging, particularly when simulation involves a multi-layer system such as a pavement section. Commercially available software, ABAQUS®, has built-in material models that can be used to simulate shrink and swell behaviors of expansive soils by accounting for moisture content and suction related changes.

The material models used in the FEM analyses are Moisture-Swelling and Sorption models. The Moisture-Swelling model defines the saturation-driven volumetric swelling of the soil matrix during partially saturated flow condition and requires volumetric strain data with changes in moisture content. The Sorption model replicates suction changes in the soil matrix with change in moisture content. The volumetric strain vs moisture content data to be input into Moisture-Swelling model was obtained by conducting 3-D volumetric strain tests that were described in the earlier paper, while the suction versus moisture content data to be input into the Sorption model was obtained by using the filter paper method described in SWCC studies. The properties used in the FEM modeling for each of the soils are presented in Table 3.

Since swell-shrink behavior of the soil is the main focus in this research, an element with swell capabilities and linear elastic properties was used for simulating a plastic clay layer. The soil element, when subjected to swelling, undergoes volumetric changes caused by absorbing water, and this element is not expected to either fail or yield during the swelling period. Consequently, a linearly elastic property was applied for all four clay material sections of this research.

A typical pavement section with a 102 mm thick asphalt layer underlain by 204 mm base layer was analyzed with 1830 mm subgrade layer. Three dimensional element types C3D8R, which are continuum stress/displacement, three-dimensional, linear hexahedron element types with no pore pressure being allowed, were used to model the asphalt and base course layers, while C3D8P elements were used for soil layer. The C3D8P elements are similar to C3D8R elements, but allow pore pressure development to replicate the soil behavior close to natural condition. The bottom most nodes in the x-z plane of the 3-D model were fixed in all directions, not allowing displacements in any direction. The surface elements in the x-y plane of the model were restricted to move in z-direction, and the surfaces in the y-z plane were restricted to move in x-direction. No lateral deformation was allowed on any of the four surfaces, and they were free to move in the vertical direction. Moisture content flow was allowed from both sides of the pavement shoulders for inducing swelling in the subsoil layers.

Figures 13 a to c present deformed mesh of the discretized pavement section built on a typical site, the Paris test site. The movements in the deformed mesh are attributed to moisture content changes from various moisture content conditions, including a saturation moisture content. As seen in Figure 13b, swell movements in a vertical direction can be clearly seen on the elements near the pavement shoulder section, as indicated by 'A'. The maximum swell

movement recorded here was 61.7 mm, which yielded to 3.43% of total swell strain. Similar analyses were attempted on other three site sections, and vertical swell strains were recorded by simulating moisture content variations that transpired in the field conditions. All these swell strain predictions were used as FEM-predicted data in the following comparison analyses.

### **Comparisons of Vertical Swell Strain Predictions**

Figure 14 presents a comparison between vertical swell strain prediction results by analytical and numerical FEM models, with measured swell strains from field elevation surveys of all four test sites. The following observations are based on the comparisons:

- Based on the measured field swell strain data, the Paris test section experienced the highest swelling-induced soil movements; whereas, the Houston test section experienced the lowest swelling amounts.
- Both PVR and Lytton models provided predictions that lie below and above the field measurements, respectively; hence, it can be stated that these two analytical models provided results that represent low and upper bound predictions of the true vertical swell-induced soil movements in the field. Overall, however, Lytton model predictions were closer to the field measurements. Low predictions by the PVR method can be attributed to coefficients used in the conversion of volumetric swell strains to vertical swell strains.
- Numerical modeling results showed similar trends as those observed in the field elevation measurements of all four sections, and these values were also close to field elevation measurements.
- The present correlation for vertical swell strain predictions showed swell strain values close to field measurements. Vertical swell strain measurements appeared to show a closer simulation since the boundary conditions in laboratory and field tests were similar.



Hence, the present vertical swell strain models can be used to estimate swell movements occurring in the field.

This second part of the analysis shows the prediction capacities of analytical and numerical models that account for moisture content variations in the analysis. The correlation developed here also provided good predictions. Overall, this analysis indicates that soil swell movements can be predicted with reasonable accuracy for civil infrastructure projects. Based on the predicted soil swell movements, necessary stiffening of the infrastructure should be attempted in new infrastructure construction, and proper remedial measures should be taken for the existing infrastructure projects.

Future research should account for a more expansive soil database with the gaps that are identified by the research presented in this paper and also address shrinkage strain movements that have received very little attention in the current state of practice.

## **SUMMARY AND CONCLUSIONS**

The following summarizes a few of the major conclusions obtained from present research results and analyses. Based on the present tests on all soils, a good correlation is noted between plasticity index and the percentage of Montmorillonite mineral content. Also, from volumetric swell tests, the ratio between vertical and volumetric swell strains was close to 0.5 ( $\frac{1}{2}$ ). This value indicates that the use of 0.33 ( $\frac{1}{3}$ ) times the volumetric swell as vertical swell strain (as assumed in PVR model) needs further scrutiny for medium-to-high plasticity (PI) soils. Laboratory vertical swell strain correlations from this study showed good correlations with plasticity index property, as these results were in close agreement with those reported by Seed et al. (1962) and Chen (1983). Shrinkage strain measurements of present soils also showed similar trends with soil properties as swell strain measurements. An attempt was made to develop

correlations between swell and shrinkage strains, with compaction moisture content changes. These correlations were later evaluated for swell-related volume change predictions. It should be noted here that further studies are necessary to reduce the scatter observed in the test results and have a better understanding on the proposed relationships.

Four field test sites, with different field boundary conditions, were monitored for their elevational changes over several months, and the monitoring data was used to evaluate several swell strain prediction models. Two analytical models provided predictions that represent low and upper bound predictions of the true swell movements in the field. The present moisture content-based swell strain correlations provided results that showed a close match with field measurements. Another numerical model, utilizing a swell-based soil model, also provided reasonable predictions of vertical swell strains.

The moisture content-based correlations appear to show good predictions of expansive soil behavior. Further research is still needed with independent soil test data to evaluate the developed correlations. Overall, the results showed that it is essential to characterize expansive soil behavior more realistically, which can lead to better and resilient civil infrastructure on expansive soils.

## **ACKNOWLEDGEMENTS**

This research was conducted in cooperation with the Texas Department of Transportation. The authors would like to acknowledge Mr. Mile Garrison, District Materials Engineer in the Atlanta District, Mr. Patrick Downey, District Pavement Engineer in the San Antonio District and Dr. Soheil Nazarian, Professor, University of Texas at El Paso for their excellent cooperation throughout the research.

## REFERENCES

- Chen, F. H., 1983. *Foundation on Expansive Soils*. Elsevier Scientific Publishing Co., New York, USA.
- Fahoum, K., Aggour, M. S. and Amini F., 1996. Dynamic Properties of Cohesive Soils Treated with Lime. *Journal of Geotechnical Engineering* 122, 382.
- Hamberg, D. J., 1985. A simplified method for predicting heave in expansive soils. M.S. thesis, Colorado State University, Fort Collins, CO.
- Hammons, M. I., 1998. *Advanced pavement design: Finite element modeling for rigid pavement joints*. Rep. No. II: Model Development, DOT/FAA/AR-97-7, Federal Aviation Administration, U.S. Dept. of Transportation.
- Kim, J., and Hjelmstad, K. D., 2003. Three-Dimensional Finite Element Analysis of Doweled Joints for Airport Pavements. *Transportation Research Record*, 1853, 100-109.
- Kodikara, J.K. and Choi, X., 2006. A simplified analytical model for desiccation cracking of clay layers in laboratory tests. *Geotechnical Special Publication*, 147, Proceedings of the Fourth International Conference on Unsaturated Soils, 2558-2569.
- Kuo, C., Huang, C., 2006. Three-dimensional pavement analysis with nonlinear subgrade materials. *Journal of Materials in Civil Engineering* 18(4), 537-544.
- Lytton, R., Aubeny, C., Bulut, R., 2004. Design procedure for pavements on expansive soils. Report No. FHWA/TX-05/0-4518-1, Texas Department of Transportation, 1-32.
- McDowell, C., 1956. Interrelationship of load, volume change, and layer thickness of soils to the behavior of engineering structures. *Proc. Highway Research Board*, No. 35, 754-770.
- Puppala, A. J., Manosuthikij, T., and Chittoori, B. C. S., 2013. Swell and Shrinkage Characterizations of Unsaturated Expansive Clays From Texas. Accepted for publication in *Engineering Geology Journal*, doi: 10.1016/j.enggeo.2013.07.001.

Seed, H.B., Woodward, R.J., and Lundgren, R., 1962. Prediction of swelling potential for compacted clays. *Journal of Soil Mechanics and Foundation Division ASCE*, 88 (3), 53-87.

## LIST OF TABLES

Table 1 Properties of the soils used in this research

Table 2 Soil swelling movements results from the laboratory empirical correlations

Table 3 Input data for Moisture-swelling and Sorption models in Finite Element Model

## LIST OF FIGURES

Figure 1a: Relationships between vertical and volumetric swell strains

Figure 1b: Relationships between slope of vertical and volumetric swell strain (AVSR) and plasticity index (PI)

Figure 2a: Relationships between vertical and volumetric shrinkage strains

Figure 2b: Relationships between Slope of Vertical & Volumetric Shrinkage Strain (AVSR) and Plasticity Index (PI)

Figure 3: Plots of vertical swell strain ( $\epsilon_{s,ver}$ ) with PI for different initial moisture conditions

Figure 4: Plots of radial swell strain ( $\epsilon_{s,rad}$ ) with PI for different initial moisture conditions

Figure 5: Plots of volumetric swell strain with PI for different initial moisture conditions

Figure 6: Depiction of vertical swell strain with PI for different correlations

Figure 7: Plots of Vertical Shrinkage Strain Versus PI of the Soil at Different Initial Compaction Moisture Contents

Figure 8: Plots of Volumetric Shrinkage Strain Versus PI of the Soil at Different Initial Compaction Moisture Contents

Figure 9: Plots between % Montmorillonite mineral content and plasticity index (PI)

Figure 10 Correlations of Swell Strains ( $\epsilon_s$ ) Versus Soil Moisture Content Change ( $\Delta w$ )

Figure 11 Correlations of Volumetric Shrinkage Strains ( $\epsilon_s$ ) Versus Soil Moisture Content Change ( $\Delta w$ )

Figure 12 Plot of elevation changes in San Antonio site

Figure 13 Typical 3-D views of pavement section showing (a) Materials and Boundary Conditions (b) Deformed elements with vertical displacement contours

Figure 14 Comparison of predicted vertical swell strains with measured vertical swell strains

**Table 1 Properties of the soils used in this research**

|                                 | <b>Fort Worth</b> | <b>San Antonio</b> | <b>Paris</b> | <b>Houston</b> | <b>El Paso</b> |
|---------------------------------|-------------------|--------------------|--------------|----------------|----------------|
| <b>Liquid Limit (LL, %)</b>     | 61                | 58                 | 60           | 54             | 30             |
| <b>Plasticity Index (PI, %)</b> | 37                | 36                 | 37           | 33             | 16             |
| <b>USCS Classification</b>      | CH                | CH                 | CH           | CH             | CL             |
| <b>% Illite</b>                 | 16                | 18                 | 13           | 26             | 63             |
| <b>% Kaolinite</b>              | 34                | 40                 | 17           | 38             | 29             |
| <b>% Montmorillonite</b>        | 50                | 42                 | 70           | 36             | 8              |

**Table 2 Soil swelling movements results from the laboratory empirical correlations**

|                                       | <b>Fort Worth</b> | <b>San Antonio</b> | <b>Paris</b> | <b>Houston</b> |
|---------------------------------------|-------------------|--------------------|--------------|----------------|
| <b>Optimum Moisture Content (%)</b>   | 24.0              | 21.7               | 23.0         | 20.0           |
| <b>Saturated Moisture Content (%)</b> | 43.3              | 43.0               | 43.3         | 35             |
| <b>Estimated Swell Movement (%)</b>   | 6.9               | 7.7                | 7.3          | 5.4            |

**Table 3 Input data for moisture-swelling and sorption models in finite element model**

|                    |            | <b>Saturation</b> | <b>Volumetric Strain (in/in)</b> | <b>Suction (Pa)</b> |
|--------------------|------------|-------------------|----------------------------------|---------------------|
| <b>Fort Worth</b>  | OMC        | 0.77              | 0.071                            | $-1.0 \times 10^6$  |
|                    | Wet of OMC | 0.95              | 0.1636                           | $-3.8 \times 10^5$  |
|                    | Saturation | 1                 | 0.2407                           | 0                   |
| <b>San Antonio</b> | OMC        | 0.7               | 0.1368                           | $-2.0 \times 10^6$  |
|                    | Wet of OMC | 0.91              | 0.2197                           | $-6 \times 10^5$    |
|                    | Saturation | 1                 | 0.2895                           | 0                   |
| <b>Paris</b>       | OMC        | 0.75              | 0.117                            | $-2.0 \times 10^6$  |
|                    | Wet of OMC | 0.96              | 0.224                            | $-6 \times 10^5$    |
|                    | Saturation | 1                 | 0.269                            | 0                   |
| <b>Houston</b>     | OMC        | 0.78              | 0.067                            | $-1.0 \times 10^6$  |
|                    | Wet of OMC | 0.93              | 0.1413                           | $-3.8 \times 10^5$  |
|                    | Saturation | 1                 | 0.2169                           | 0                   |

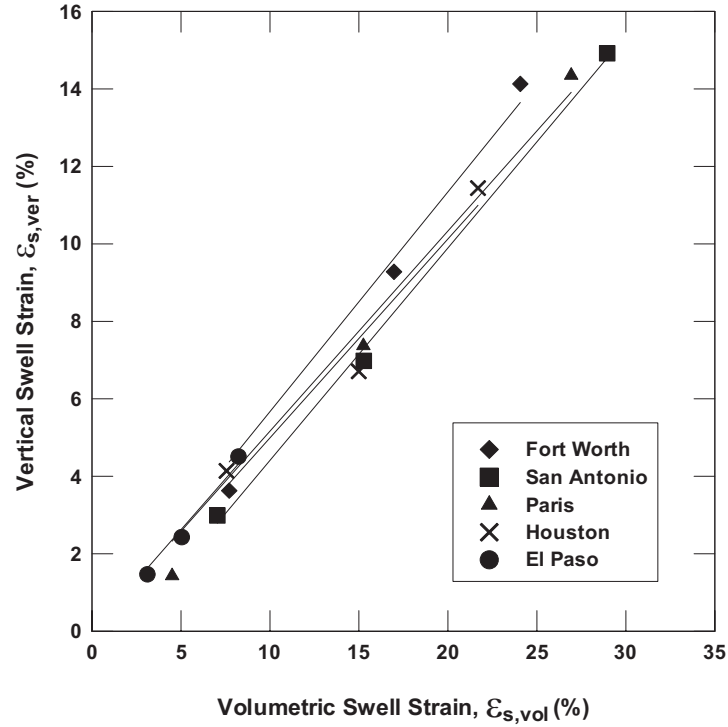


Figure 1a: Relationships between vertical and volumetric swell strains

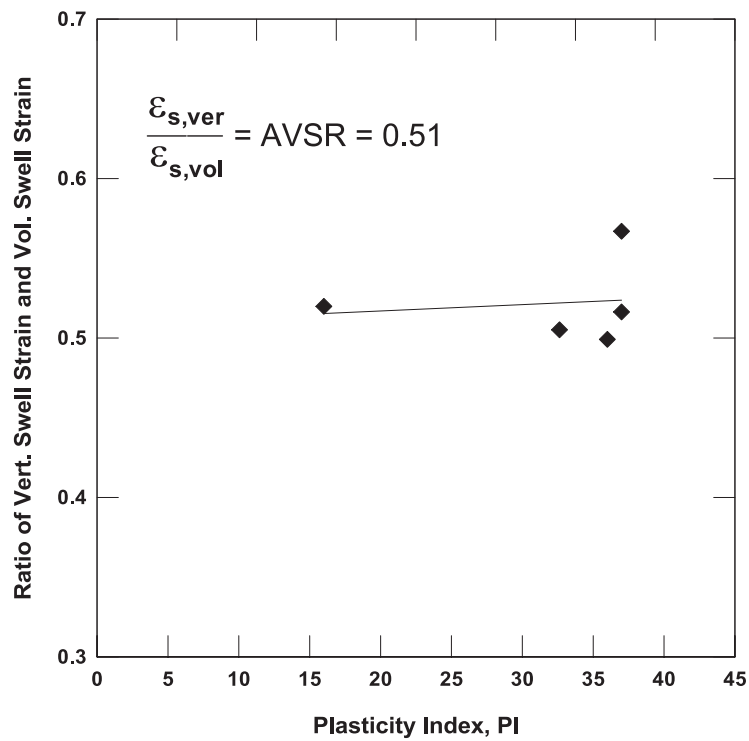


Figure 1b: Relationships between slope of vertical and volumetric swell strain and plasticity index (PI)



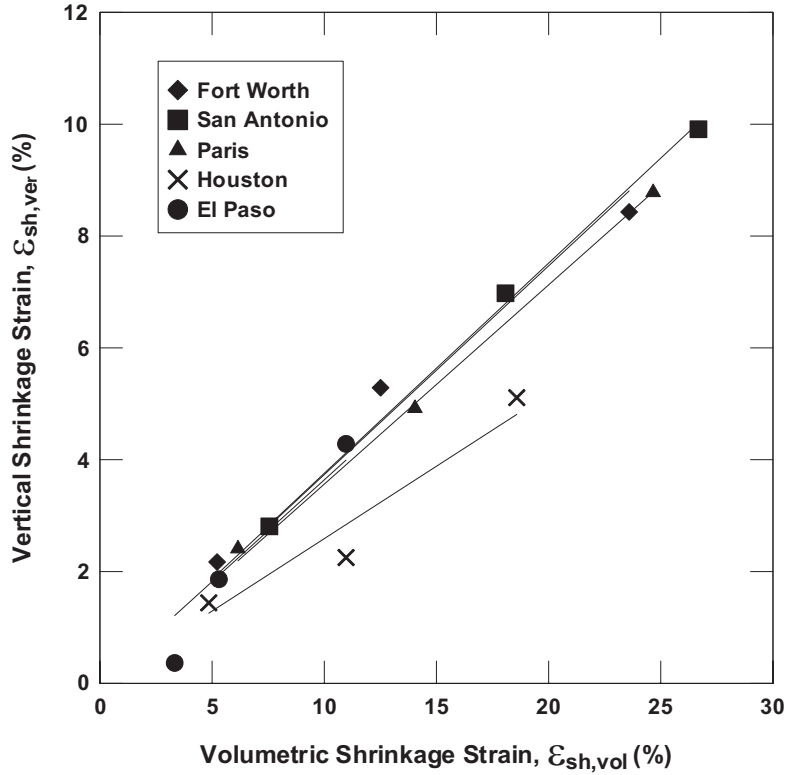


Figure 2a: Relationships between vertical and volumetric shrinkage strains

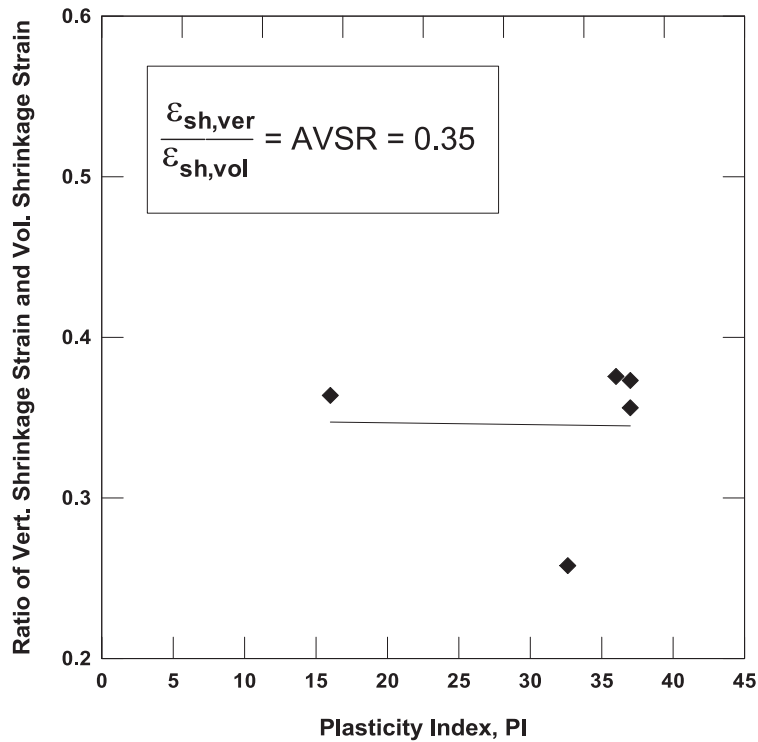


Figure 2b: Relationships between Slope of Vertical & Volumetric Shrinkage Strain and Plasticity Index (PI)

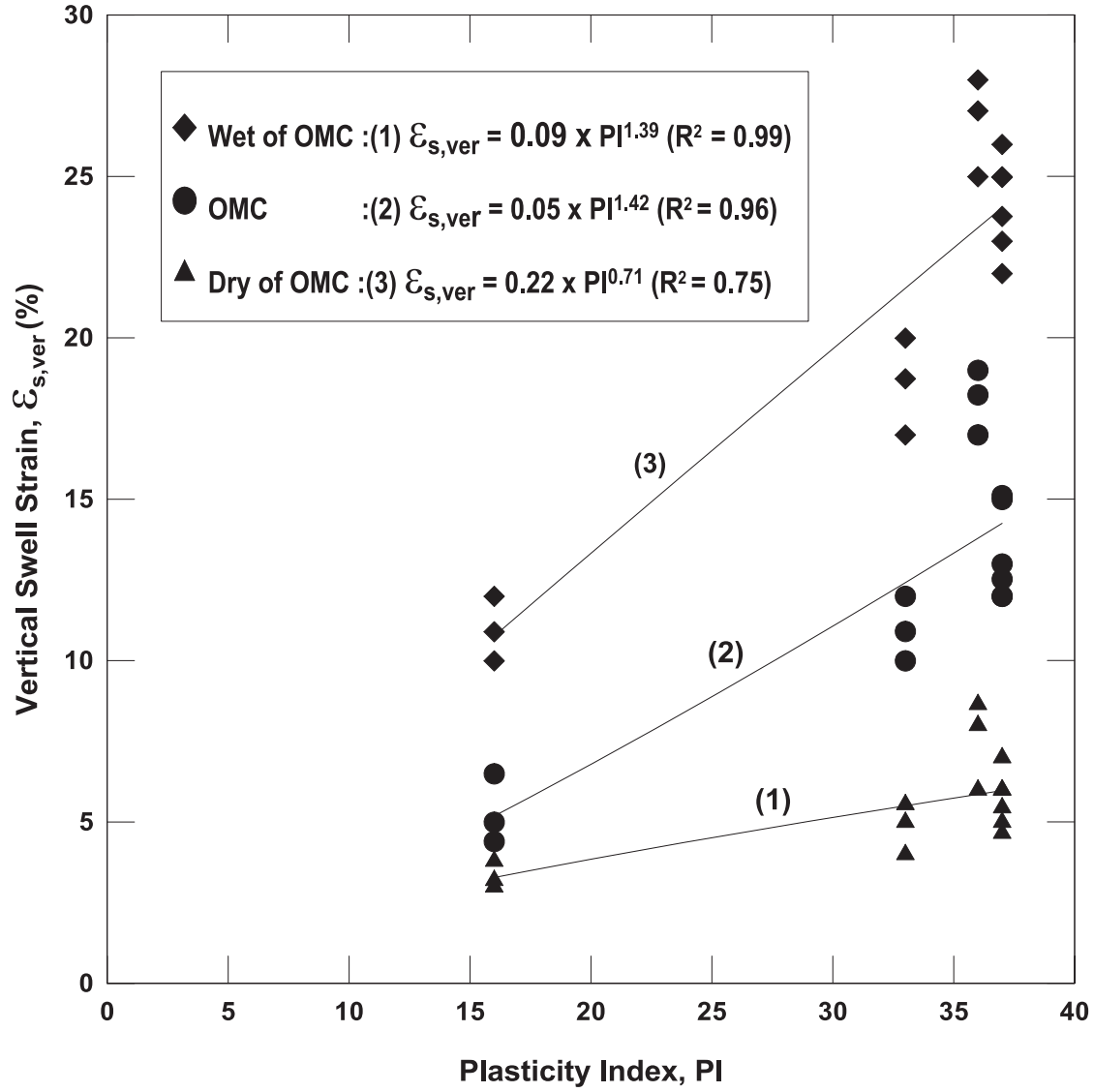


Figure 3: Plots of vertical swell strain ( $\epsilon_{s,ver}$ ) with PI for different initial moisture conditions

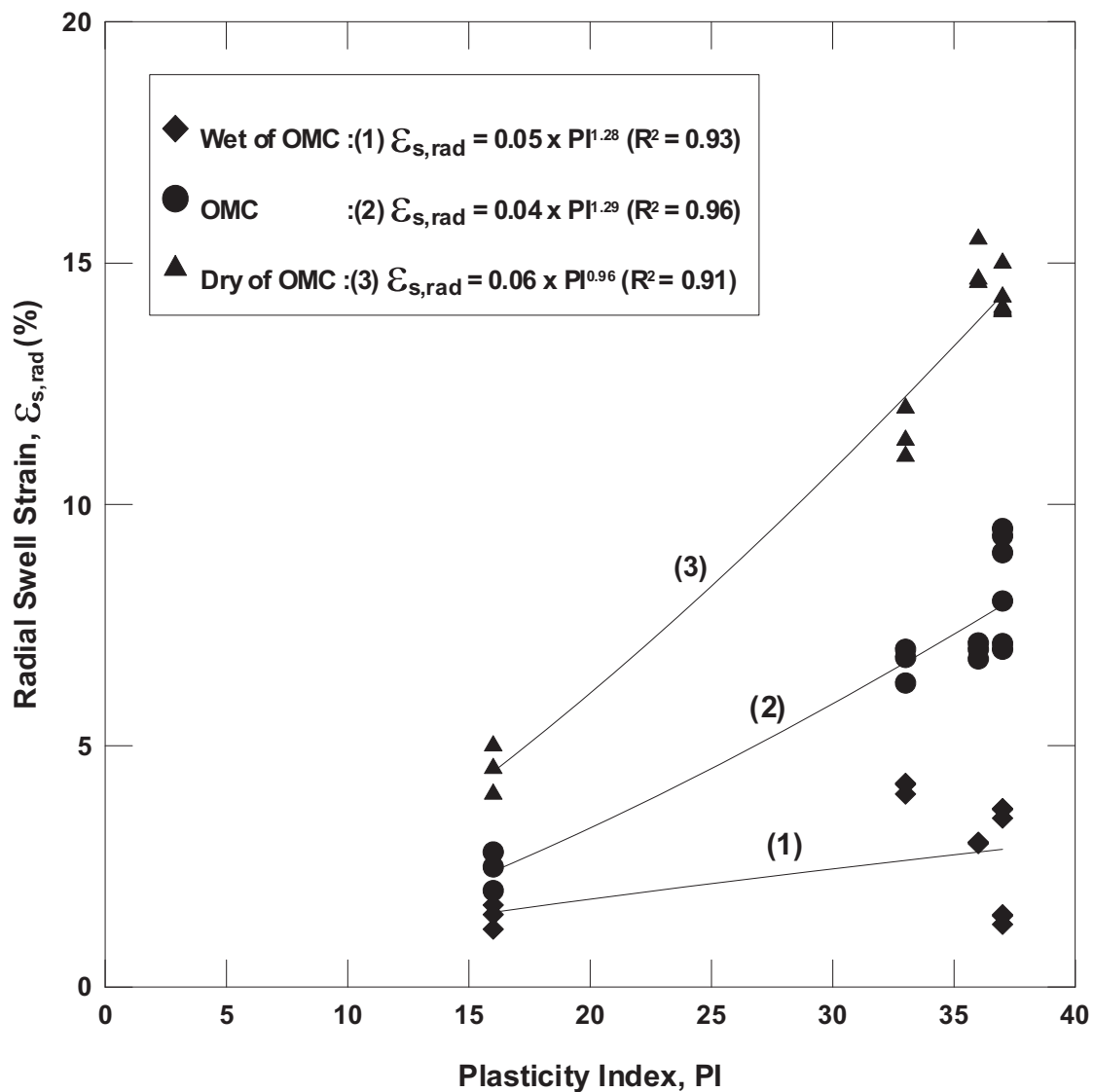


Figure 4: Plots of radial swell strain ( $\epsilon_{s,rad}$ ) with PI for different initial moisture conditions

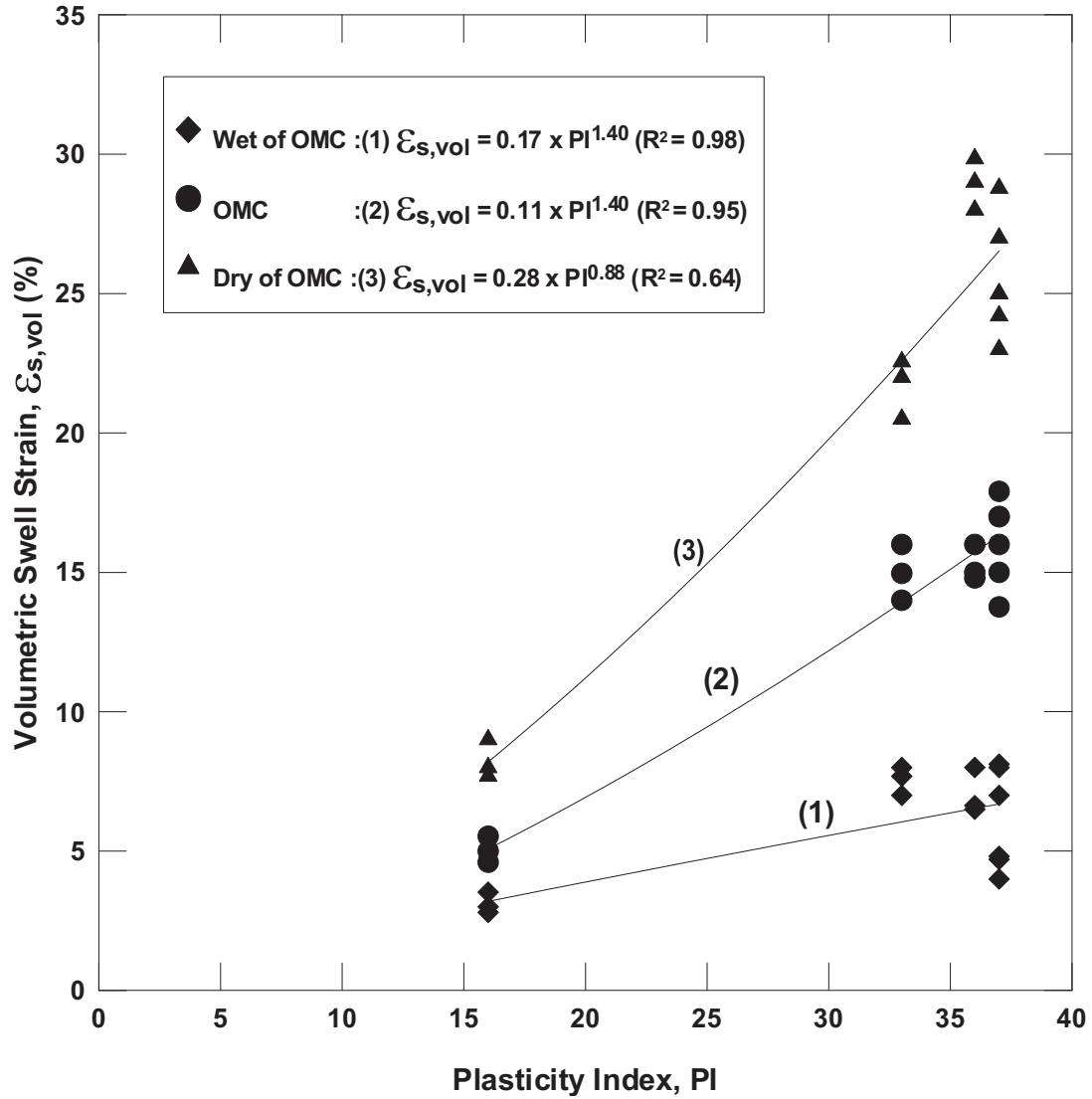


Figure 5: Plots of volumetric swell strain with PI for different initial moisture conditions

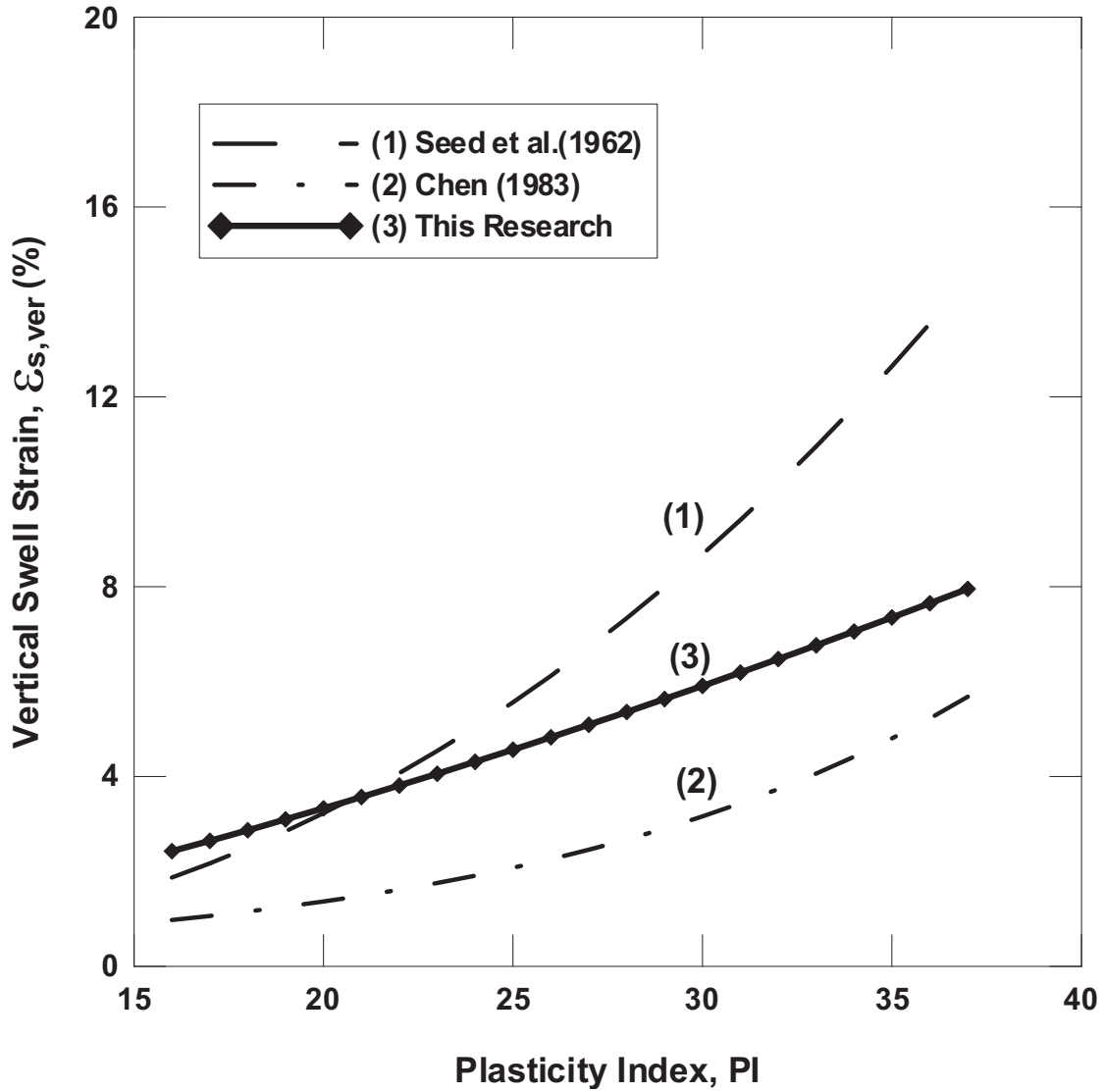
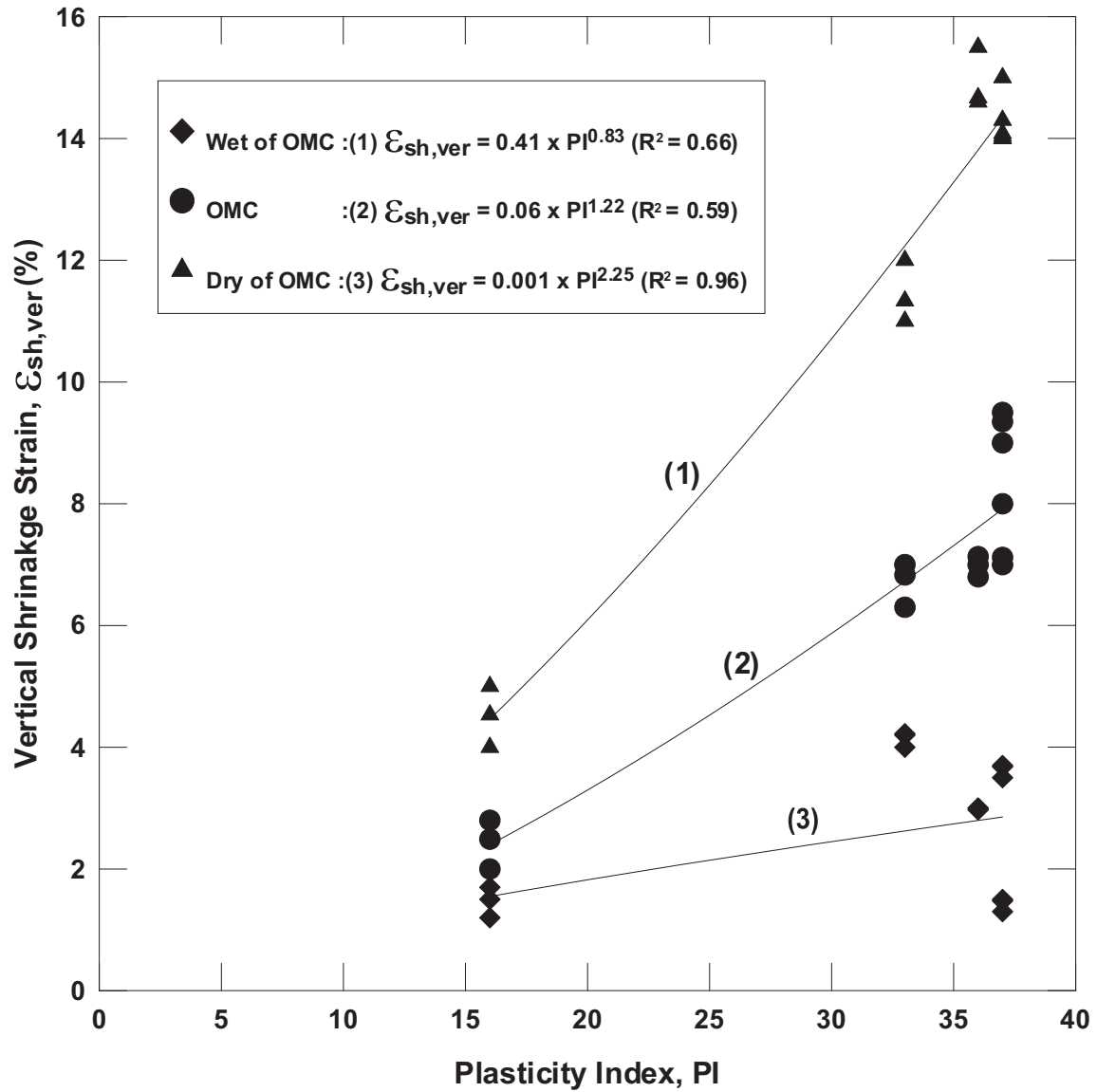
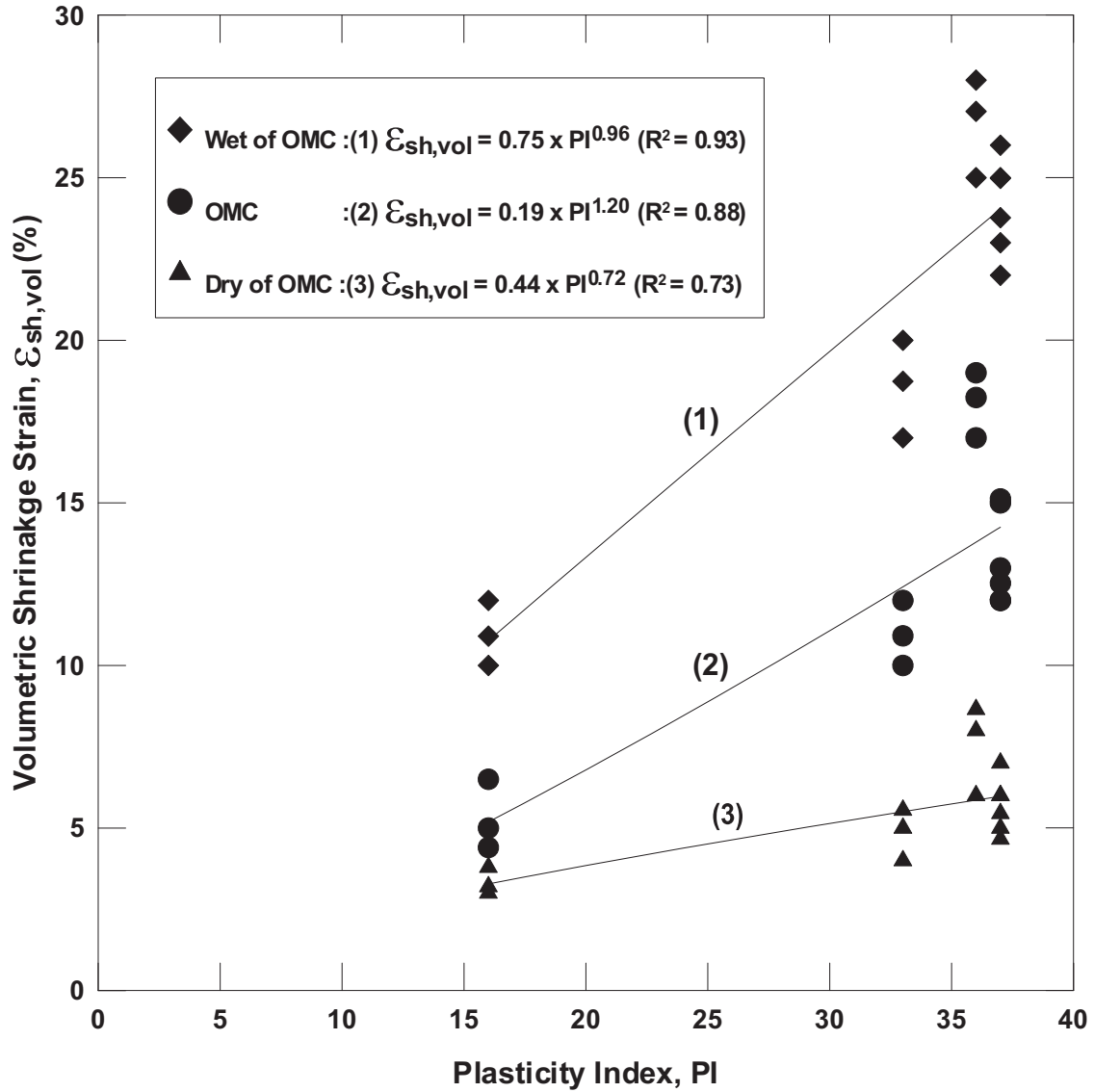


Figure 6: Depiction of vertical swell strain with PI for different correlations



**Figure 7: Plots of Vertical Shrinkage Strain Versus PI of the Soil at Different Initial Compaction Moisture Contents**



**Figure 8: Plots of Volumetric Shrinkage Strain Versus PI of the Soil at Different Initial Compaction Moisture Contents**

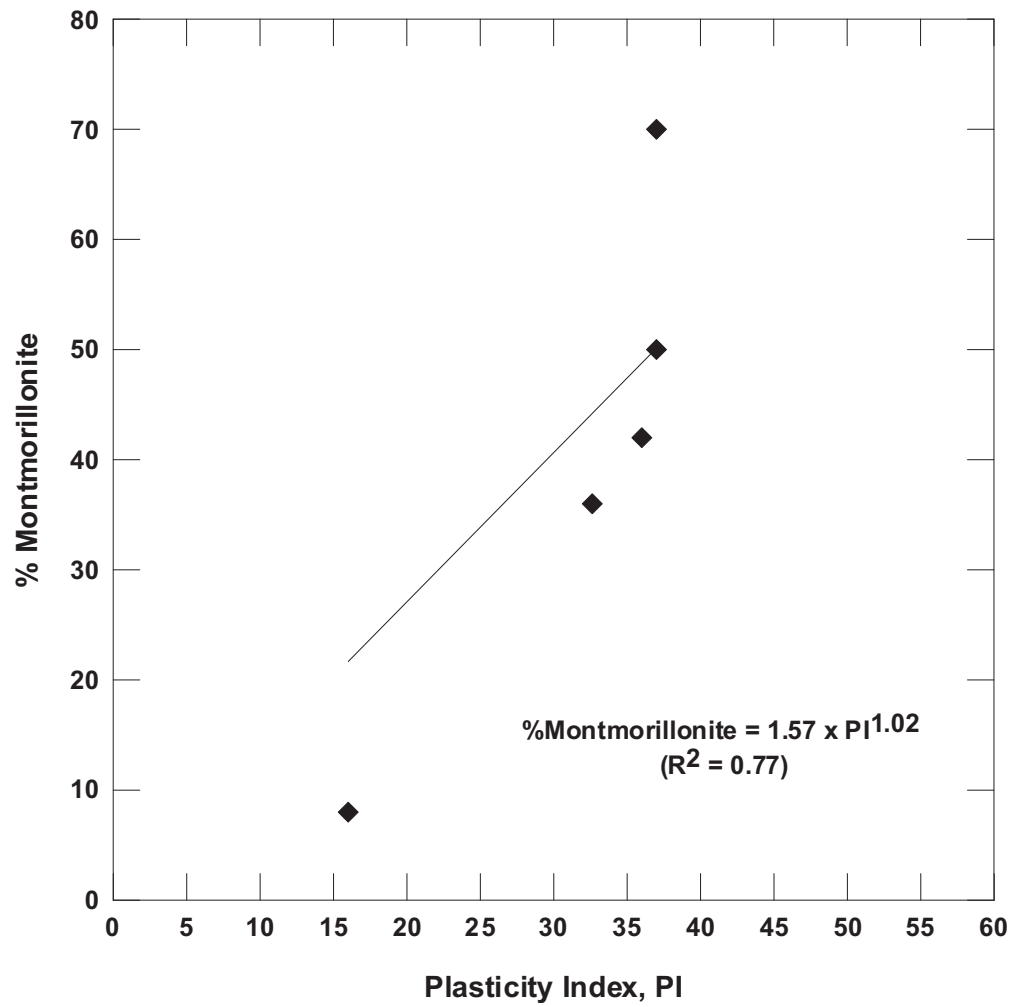


Figure 9: Plots between % Montmorillonite mineral content and plasticity index (PI)



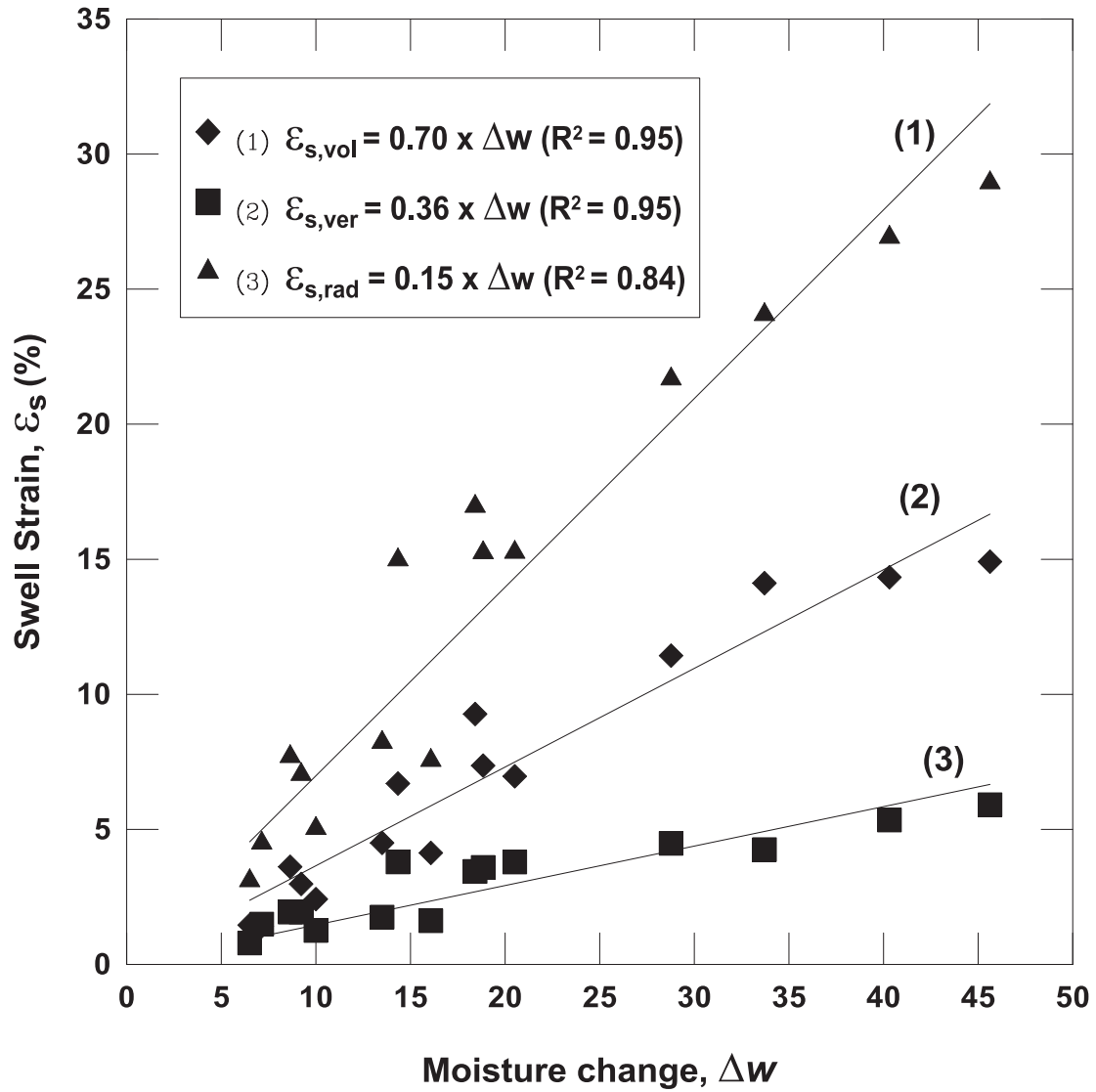


Figure 10 Correlations of Swell Strains ( $\epsilon_s$ ) Versus Soil Moisture Content Change ( $\Delta w$ )

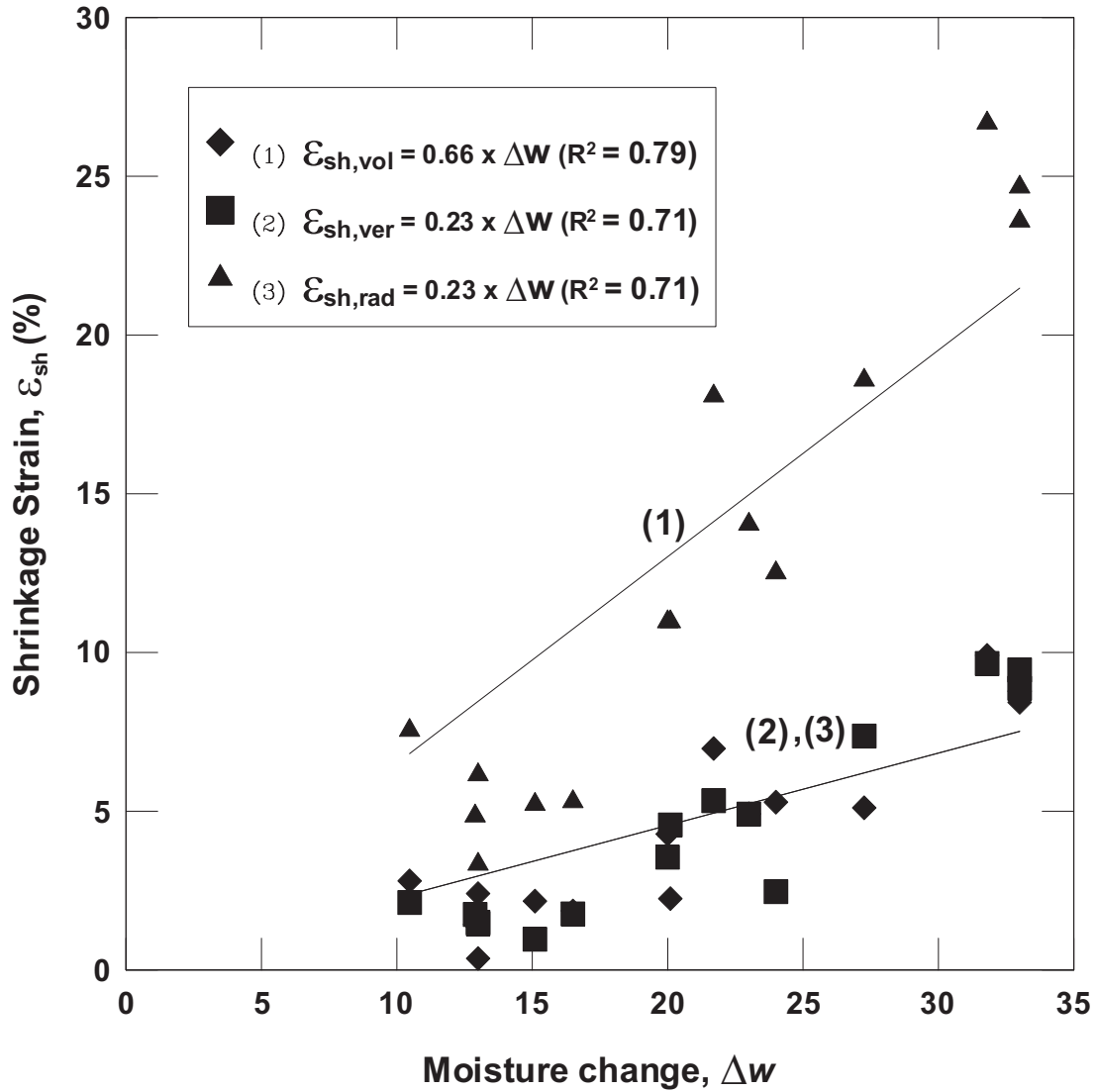


Figure 11 Correlations of Volumetric Shrinkage Strains ( $\epsilon_s$ ) Versus Soil Moisture Content Change ( $\Delta w$ )

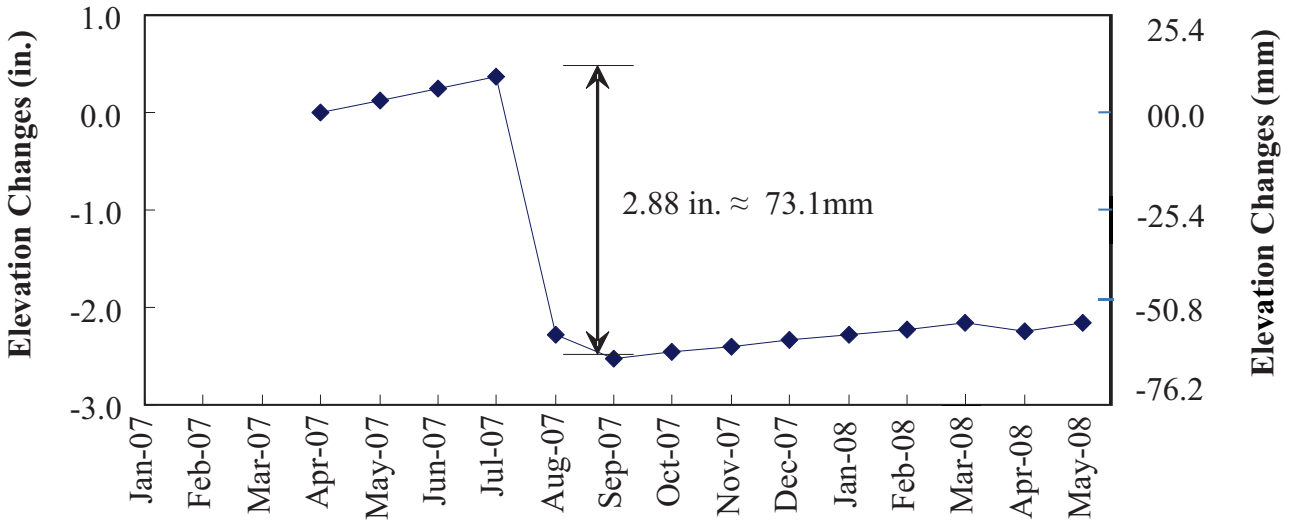
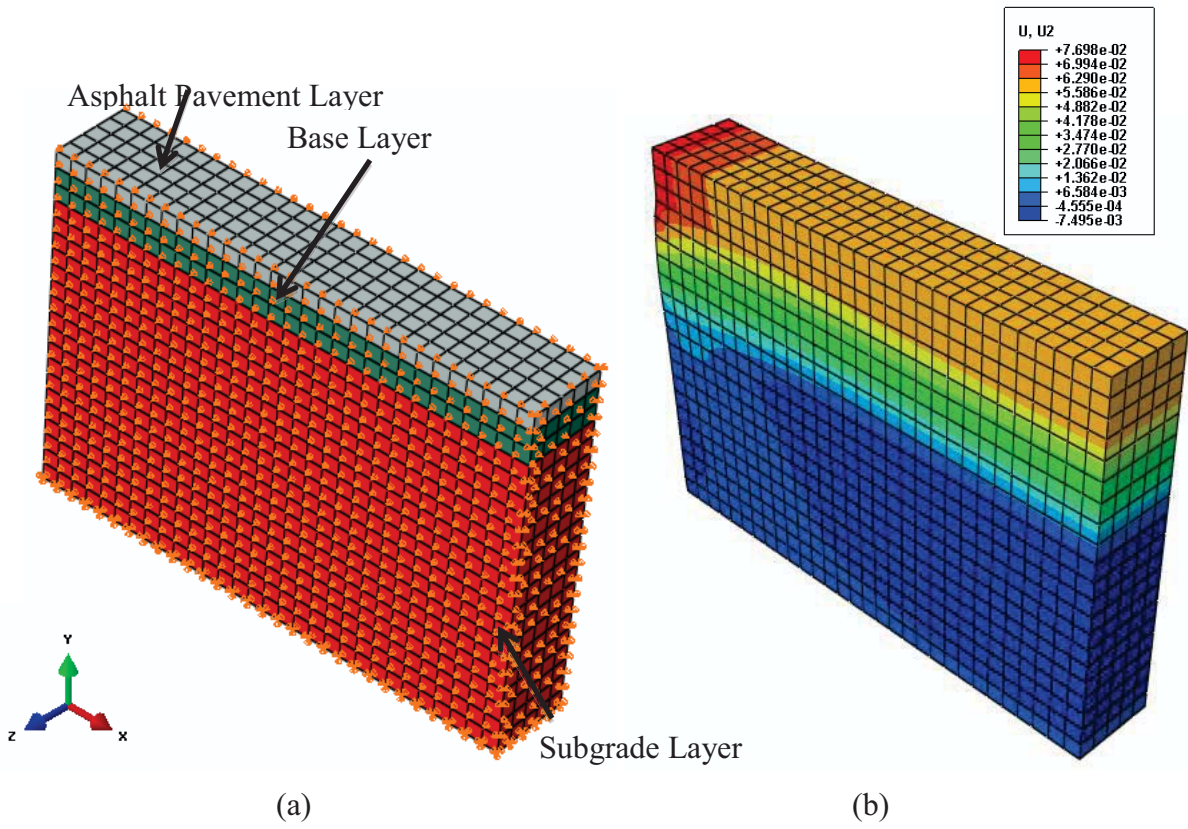


Figure 12 Plot of elevation changes in San Antonio site



**Figure 13 Typical 3-D views of pavement section showing (a) Materials and Boundary Conditions (b) Deformed elements with vertical displacement contours**

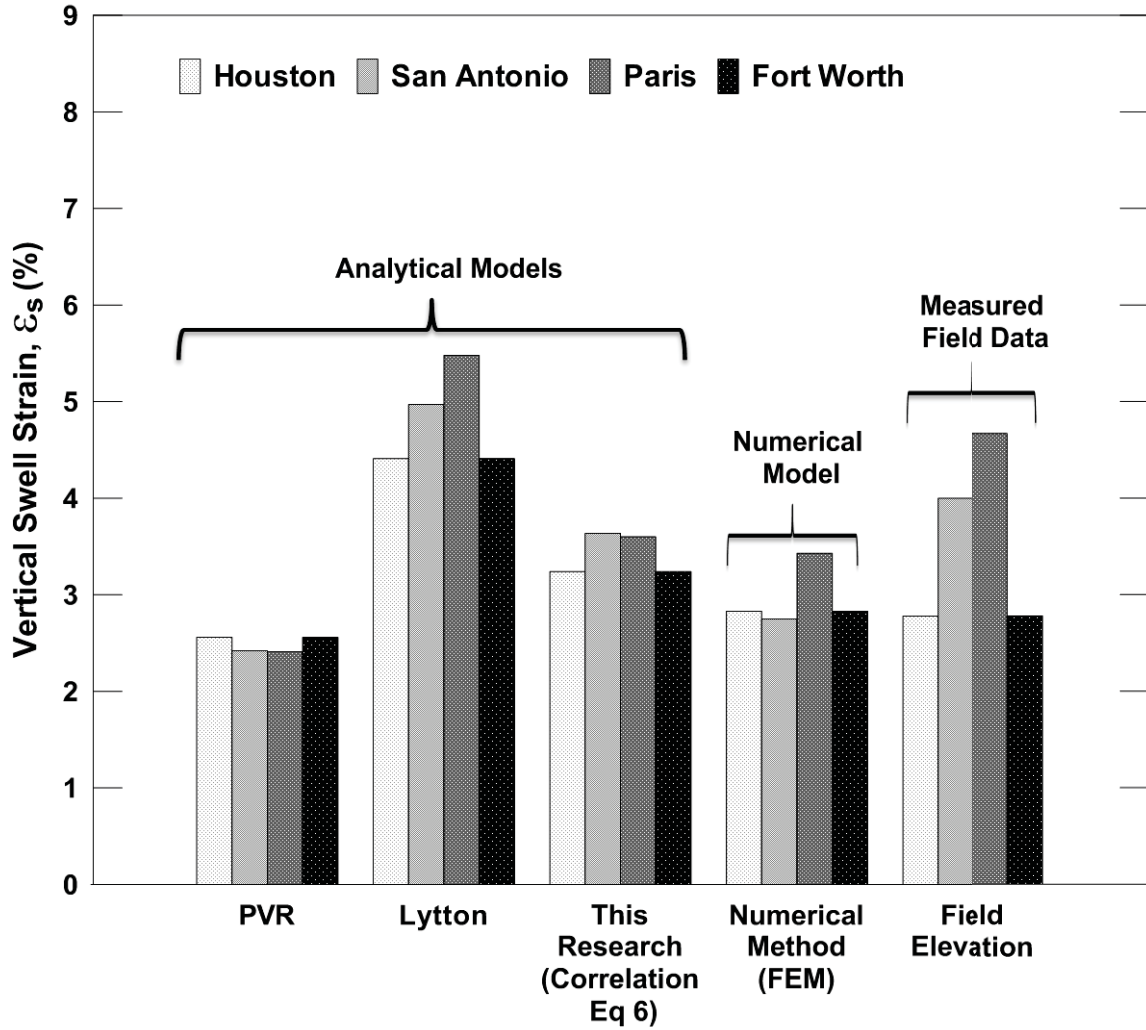


Figure 14 Comparison of predicted vertical swell strains with measured vertical swell strains

### **Research Highlights**

- Analytical models were developed for swell and shrink prediction in expansive soils
- New models were developed for predicting swelling and shrinkage in expansive soils
- Comparison analysis was made between new and old models for validation
- Models with test procedural information and moisture content variations predict well